Deterministic dynamics of stimulated scattering phenomena with external feedback

Weiping Lu, A. Johnstone, and R. G. Harrison
Department of Physics, Heriot-Watt University, Edinburgh EH14 4AS, United Kingdom
(Received 16 March 1992)

A reasonably complete theoretical description of stimulated scattering in the presence of low-reflectivity external feedback is presented, based on an earlier treatment by Lu and Harrison [Europhys. Lett. **16**, 655 (1991)] generalized to account for the integral effect of nonlinear refraction. Theoretical results show the Stokes signal to exhibit huge sustained or random bursts of quasiperiodic emission. Detailed comparisons with experimental findings on stimulated Brillouin scattering generated in single-mode optical fiber with weak external feedback by continuous-wave excitation give good agreement regarding both the dynamical features of the Stokes emission and their dependence on the physical control parameters, e.g., pump power, cavity reflectivity, and fiber length. Significantly, our results confirm the essential role of nonlinear refraction to the dynamical behavior and suggest that the noise structure of the initial spontaneous scattering has little influence on this behavior.

PACS number(s): 42.65.Es

I. INTRODUCTION

Stimulated scattering is a fundamental nonlinear process in which a frequency down-shifted scattered (Stokes) signal is generated from the interaction of a pump signal with a material wave. Here the usual triad-resonance condition involving the wave vectors of the individual electromagnetic and appropriate material waves, with their own dispersion relations dictate the scattering direction and the frequency of the scattered wave. Conventional mathematical treatments of stimulated scattering [1] are truncated descriptions in the sense that the integral effects of field- (pump and Stokes) induced nonlinear refraction are omitted. While such analysis is justified on the basis of steady-state operation Lu and Harrison have recently shown [2] in a more complete treatment that the interplay of nonlinear refraction with the gain of these processes leads to rich dynamical instabilities and chaos in the scattered and pump fields. Omissions of dispersive effects resulted in stable emission only, via transient relaxation oscillations [3]. Such behavior is shown to be prevalent over broad experimentally accessible operating conditions, in some instances from the onset of stimulated scattering. It has been further shown in other theoretical work [4–6] that the inclusion of noise in the spontaneous scattering leads to fluctuation of a stochastic nature in the stimulated scattering.

In the light of recent well-defined experiments on stimulated Brillouin scattering (SBS) in optical fiber [2(a),7,8], confirming rich aperiodic behavior in the emission, the relative roles of nonlinear dispersion and noise in determining this behavior is an outstanding issue of some importance. Toward clarifying the role of nonlinear refraction, in this paper we consider stimulated scattering in the presence of weak external feedback. Our experimental findings so far for SBS in a single-mode fiber with continuous-wave excitation (see also Refs. 7 and 9) show a dramatic modification of the dynamics to sustained and bursting modes of quasiperiodic behavior, the distinct features of which, along with their different operating conditions, provide an excellent basis for quantitative tests of our mathematical description. No evidence is found for sustained stable emission.

Our results, which are shown to be in good accord with the predictions of this generalized treatment, confirm the essential role of nonlinear refraction on the dynamical behavior of this scattering process. Here effects of noise of the spontaneous scattering therefore appear to have little influence on the deterministic behavior. Further, the omission of refractive effects results only in periodic emission in agreement with earlier work [10,11], although we find such dynamics to exist only close to threshold, the emission otherwise being stable. In the limit of very high cavity feedback, not considered here, other analysis has nevertheless provided evidence of chaotic emission [12].

II. THEORETICAL DESCRIPTION

Stimulated scattering results from nonlinear coupling between two optical waves and an acoustic wave. The optical waves, namely pump and Stokes, are governed by the couped wave equations,

$$\begin{aligned}\nabla\times\nabla\times\mathbf{E}_1+\frac{n^2}{c^2}\frac{\partial^2}{\partial t^2}\mathbf{E}_1=\mu_0\omega^2\mathbf{P}^{\mathrm{NL}}(\omega_1)\ ,\\ \nabla\times\nabla\times\mathbf{E}_2+\frac{n^2}{c^2}\frac{\partial^2}{\partial t^2}\mathbf{E}_2=\mu_0\omega^2\mathbf{P}^{\mathrm{NL}}(\omega_2)\ ,\end{aligned}\tag{1}$$

where $\mathbf{E}_1$ and $\mathbf{E}_2$ are the amplitudes of the pump and Stokes fields of frequency ω_1 and ω_2, respectively. The material wave, driven by the two optical beams, obeys a general equation of the form

$$\left[\frac{\partial^2}{\partial t^2}-2\Gamma\frac{\partial}{\partial t}-v^2\nabla^2\right]M=-\nabla\cdot\mathbf{f}\ ,\tag{2}$$

where M is the material-wave field amplitude, v is its velocity, and Γ the damping coefficient of the wave or the

half-width of the associated spontaneous scattering spectrum. For a complete description, the nonlinear polarization $\mathbf{P}^{\mathrm{NL}}(\omega)\equiv\mathbf{P}^{(3)}(\omega)$ contains, in general, two parts

$$\mathbf{P}^{(3)}(\omega)=\mathbf{P}_R^{(3)}(\omega)+\mathbf{P}_{\mathrm{NR}}^{(3)}(\omega)\ , \tag{3}$$

The first term of the right side is a resonant part and the second is a nonresonant part. They are responsible for energy transfer and refractive-index change in the interaction, respectively.

We first consider the resonant part of the polarization. This part and the driving force arise from the nonlinear coupling of the three waves and can be obtained as follows:

$$\begin{aligned}&\mathbf{P}_R^{(3)}(\omega_1)=\gamma_1 M\mathbf{E}_2\ ,\\ &\mathbf{P}_R^{(3)}(\omega_2)=\gamma_2 M^*\mathbf{E}_1\ ,\\ &\mathbf{f}=\gamma_3\nabla(\mathbf{E}_1\cdot\mathbf{E}_2^*)\ ,\end{aligned} \tag{4}$$

where γ_1, γ_2, and γ_3 are coupling constants related to the electrostrictive coefficient of the medium. Equation (4) is the same as in the conventional treatment [1].

Contributions to the nonresonant part of the nonlinear polarization arise from optical-field-induced refractive-index changes by both the pump and Stokes signals. A number of physical mechanisms can contribute [1], e.g., electronic, arising from distortion of electron distribution, electrostrictive, arising from increase in density of the medium, etc. Restricting our consideration to cw pump conditions, adiabatic elimination of the change of refractive index is a good approximation. We then obtain the general form

$$\begin{aligned}&\mathbf{P}_{\mathrm{NR}}^{\mathrm{NL}}(\omega_1)=\varepsilon_0\chi_{\mathrm{eff}}^{(3)}(|\mathbf{E}_1|^2+2|\mathbf{E}_2|^2)\mathbf{E}_1\ ,\\ &\mathbf{P}_{\mathrm{NR}}^{\mathrm{NL}}(\omega_2)=\varepsilon_0\chi_{\mathrm{eff}}^{(3)}(|\mathbf{E}_2|^2+2|\mathbf{E}_1|^2)\mathbf{E}_2\ ,\end{aligned} \tag{5}$$

where $\chi_{\mathrm{eff}}^{(e)}$ is the effective third-order susceptibility responsible for the change of refractive index. The factor 2 in the cross terms arises from mathematical derivation.

In the slowly varying approximations, the rapidly varying part of the electric and acoustic fields can be separated by writing them in the form

$$\begin{aligned}&E_1=\hat{e}_1(E_e^{-i(\omega_p t-k_p z)}+\mathrm{c.c.})\ ,\\ &E_2=\hat{e}_2(E_s e^{-i(\omega_s t+k_s z)}+\mathrm{c.c.})\ ,\\ &M=Ae^{-i(\omega_a t-k_a z)}+\mathrm{c.c.}\ ,\end{aligned} \tag{6}$$

where $\omega_p(k_p)$, $\omega_s(k_s)$, and $\omega_a(k_a)$ are the frequencies (wave vectors) of pump, Stokes, and acoustic fields, respectively, and we consider the usual case of back-stimulated scattering; that is counterpropagating pump and Stokes waves. We note that a plane-wave assumption of pump and Stokes fields is made in our treatment. This is usually a good approximation for a single-mode optical fiber. By substituting Eqs. (5) and (6) into Eqs. (1) and (2) and using the slowly varying and plane-wave approximations we obtain the reduced set of equations describing the interaction

$$\begin{aligned}&\frac{\partial E}{\partial t}+\frac{c}{n}\frac{\partial E}{\partial z}-\frac{in_2\omega}{n}(|E|^2+2|E_s|^2)E+\frac{\alpha}{2}E=iV_1E_sA\ ,\\ &\frac{\partial E_s}{\partial t}-\frac{c}{n}\frac{\partial E_s}{\partial z}-\frac{in_2\omega}{n}(|E_s|^2+2|E|^2)E_s+\frac{\alpha}{2}E_s\\ &\qquad=iV_2EA^*\ ,\\ &\frac{\partial A}{\partial t}+v\frac{\partial A}{\partial z}+\alpha_A A=iV_3EE_s^*\ ,\end{aligned} \tag{7}$$

where α is the absorption coefficient of the pump and Stokes fields and α_A the damping coefficient of the material wave, both of which are introduced phenomenologically. V_1, V_2, and V_3 are the optomaterial coupling coefficients, which are related to γ_1, γ_2, and γ_3, respectively. n_2, which is associated with $\chi^{(3)}$, is the nonlinear refractive coefficient and obeys the relation $\delta n=n_2|E|^2$. For stimulated Brillouin scattering (SBS) in optical fibers, the experimental system studied below, $V_1=V_2=\pi n^2\rho_{12}c/\lambda\rho_0$, $V_3=\pi n^5\rho_{12}\varepsilon_0/2\lambda v$, where ρ_{12} is the longitudinal elasto-optic coefficient, ρ_0 is the average density and ε_0 the free-space permittivity. Furthermore, to obtain the above equations we assume that the frequency of the acoustic wave ω_a is much lower than the pump and Stokes frequencies, e.g., $\omega_a\ll\omega_p,\omega_s$, and the interaction occurs under phase-matching conditions $k_a=k_p+k_s$. These assumptions are indeed valid in the optical fiber experiments we report.

Returning to Eq. (7), we note that the nonlinear refraction, which is described by the third terms in the first and second equations, gives rise to self-phase modulation (SPM) and cross-phase modulation (XPM) of the pump and Stokes fields [13]. We find that while the omission of such terms in conventional descriptions gives the same general steady-state intensity behavior as for our complete model description, the two differ dramatically in regard to the time-dependent features of the process. More precisely the inclusion of these additional terms results in temporally and spatially dependent variation of the phase of both pump and Stokes signals, and through this, provides the basis for the emergence of dynamical instabilities [2].

For theoretical and numerical analysis we normalize the above variables as follows:

$$\varepsilon=\frac{E}{E_0},\quad \varepsilon_s=\frac{E_s}{E_0},\quad B=\frac{iA}{E_0^2}\frac{\alpha_A}{V_3}\ . \tag{8}$$

Equation (7) then becomes

$$\begin{aligned}&\frac{\partial\varepsilon}{\partial\tau}+\frac{\partial\varepsilon}{\partial\xi}-iu(|\varepsilon|^2+2|\varepsilon_s|^2)\varepsilon+\frac{\beta}{2}\varepsilon=-g\varepsilon_sB\ ,\\ &\frac{\partial\varepsilon_s}{\partial\tau}-\frac{\partial\varepsilon_s}{\partial\xi}-iu(|\varepsilon_s|^2+2|\varepsilon|^2)\varepsilon+\frac{\beta}{2}\varepsilon=g\varepsilon_sB^*\ ,\\ &\frac{1}{\beta_A}\frac{dB}{d\tau}+B=\varepsilon\varepsilon_s^*\ ,\end{aligned} \tag{9}$$

where the parameters are

$$\tau=\frac{ct}{nL},\quad \xi=z/L,\quad u=\frac{n_2\omega L}{c}|E_0|^2,$$
$$\beta=\alpha\frac{nL}{c},\quad \beta_A=\alpha_A\frac{nL}{c},\quad g=\frac{V_1V_3nL}{\alpha_A c}|E_0|^2.$$

L is the interaction length, E_0 the pump field amplitude at $\xi=0$ (entrance end of the medium), and g is the normalized small-signal amplitude gain of the stimulated scattering. Equations (9) are our working equations that govern the steady-state and dynamical behavior of the stimulated scattering.

We now consider the boundary conditions. Since consideration is restricted in this paper to a weak-reflectivity limit, namely $R_1,R_2\ll 1$, where R_1,R_2 are the intensity reflectivities of the entrance and exit faces of the medium, the reflected field intensity from both ends is weak so that interaction with the initial pump and Stokes fields already present in the interaction length can be neglected. Furthermore the reflected pump, collinear with the incident pump, undergoes two reflections and is also neglected. For these conditions the boundary conditions become

$$\begin{aligned}\varepsilon_{s,r}(t,\xi=0)&=\sqrt{R_1}\varepsilon_s(t,\xi=0),\\ \varepsilon_s(t,\xi=L)&=\sqrt{R_2}\varepsilon_{s,r}(t,\xi=L),\end{aligned}\tag{10}$$

where $\varepsilon_{s,r}$ is the forward-propagating Stokes signal component of the stimulated scattering signal reflected by the entrance end, the evolution of which is given by the equation

$$\frac{\partial\varepsilon_{s,r}}{\partial\tau}+\frac{\partial\varepsilon_{s,r}}{\partial\xi}=-\tfrac{1}{2}\beta\varepsilon_{s,r}+iu(2|\varepsilon|^2+|\varepsilon_s|^2)\varepsilon_{s,r}.\tag{11}$$

We should note that with external feedback the Stokes output can no longer be seen as amplification of the spontaneous noise signal through a single pass of the interacting medium. Rather, the output generally depends on not only the present but also the earlier interaction process. Consequently, the noise influence on the Stokes output, for oscillator systems in general, is expected to be considerably reduced. Furthermore due to signal enhancement by the external cavity, the threshold for the Stokes signal in this case is substantially lower than that in an unbounded system as is the pump intensity for saturation of the Stokes emission.

III. DYNAMICS AND ITS PHYSICAL MECHANISMS

The essential role of nonlinear refraction and its interplay with the nonlinear gain of stimulated scattering in promoting dynamical behavior was recently demonstrated by Lu and Harrison [2]. For systems in the presence of external feedback, consideration must also be given to the effective memory imposed on the scattering processes by the feedback signals. The dynamical features in a simple system of this kind, namely stimulated Brillouin scattering in optical fibers with weak boundary, was first studied, we believe, by Bar-Joseph and collaborators in the absence of nonlinear refraction [11]. While theoretical results showed agreement with experimental findings of sustained and relaxation oscillatory features of the Stokes signal (see also Ref. [10]), the faster and more complicated dynamical behavior observed could not be explained by their conventional analysis.

To elucidate the role of feedback and nonlinear refraction on the dynamical behavior, we first compare stimulated scattering for three different cases, namely, (i) with nonlinear refraction but without feedback, (ii) with feedback but without nonlinear refraction, and (iii) with nonlinear refraction and feedback. We have numerically integrated the coupled nonlinear equations (9) and (11) in both space and time in the presence of the boundary conditions (10) by using the method of characteristics. For convenience the parameter set, which is fixed throughout, is chosen to be slightly above the threshold for stimulated scattering in the unbounded system of case (1). For this case, since the pump intensity for this parameter set is weak, the nonlinear refraction, (based, for example, on the electronic contribution for glass) is small enough to inhibit sustained dynamical behavior in the absence of the cavity and the emission evolves into a weak and stable signal through a relaxation oscillation. This is a limiting case of the general dynamical behavior discussed in Ref. [2].

For the case of the bounded systems [case (ii)] we consider a cavity with reflectivity 4% on either end of the medium corresponding in practice to a typical natural

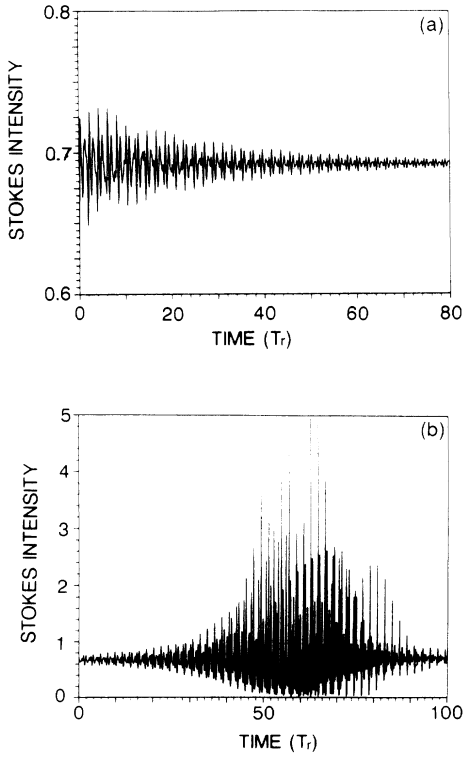

FIG. 1. (a) Relaxation oscillations of Stokes intensity, resulting from the interaction of gain with external feedback in the absence of refraction. (b) Bursting oscillation of Stokes signal in the presence of gain, refraction, and cavity feedback. The parameters are held at $g=11.4$, $\beta=0.184$, $\beta_A=90$, $u=0$, and $R_1=R_2=4\%$ with $u=0$ for trace (a) and $u=0.34$ for trace (b).

reflectivity for glass. In contrast with normal stimulated scattering, that is, without feedback, for which the initial Stokes signal can be regarded as an injection signal placed at the rear end of the medium, the Stokes signal in a feedback system, as discussed above, comprises the nonlinear amplification of an earlier signal of the interacting processes subsequently reflected by the external cavity. As a result, the cavity effect may provide an additional memory to the stimulated scattering process. Furthermore, in this case the energy conversion from the pump to the Stokes signal is increased considerably due to signal enhancement in the cavity. For this system in the absence of nonlinear refraction the temporal dynamics of the scattered signal is not sustained, but decays eventually to a stable output as shown in Fig. 1(a). We note that this system is similar to that described by Bar-Joseph [11], and the relaxation oscillation we observe is in accord with their findings, the more complicated transient dynamical features of our data arising from the noninstantaneous response of the interacting medium which we have considered in our theory. More generally our analysis shows such behavior to always prevail for operation well above the threshold for stimulated scattering and not to be noticeably sensitive to the choice of parameter values. Only close to threshold are sustained oscillations obtained. These show pure limit-cycle behavior of a period equal to twice the round-trip time of the feedback cavity $2T_r$ consistent with earlier findings [10–12].

We now consider our more complete description of stimulated scattering with feedback, [case (iii)], governed by Eqs. (9)–(11) in which the influence of nonlinear refraction is accounted for. We note that in this case the cavity provides a feedback signal not only containing intensity, as in case (ii), but also phase information. The latter may be of special importance in promoting dynamical emission, even if it is very weak, since the cavity provides an accumulative effect for the phases of the waves. Indeed, a dramatically different type of dynamical behavior, consisting of an infinite chain of intermittent oscillatory bursts with different shapes and durations, is found. An example of one of the bursts is shown in the data of Fig. 2(b) as a prelude to the detailed investigations presented below. It must therefore follow that sustained dynamical behavior of this kind results from the combined action of the nonlinear refraction with feedback, the absence of one or the other, as above, leading only to relaxation oscillation for this parameter set.

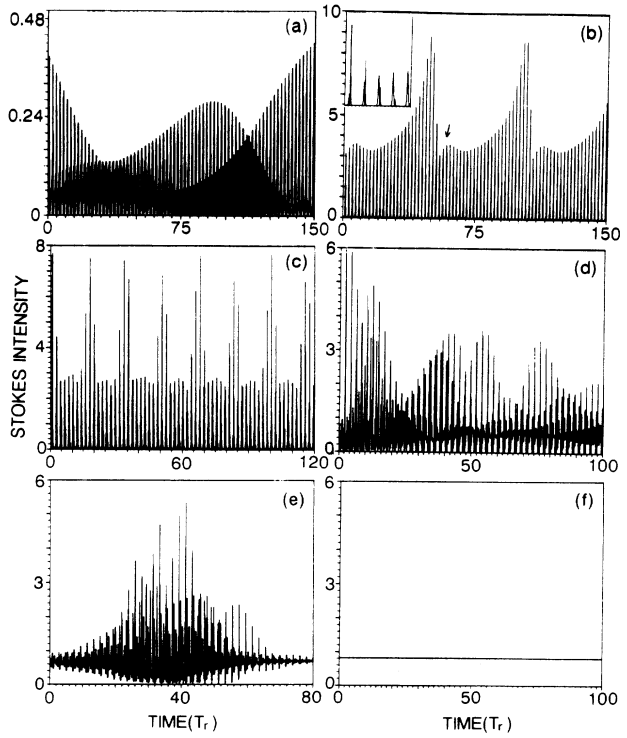

FIG. 2. A series of different dynamical features of Stokes signals on increasing pump power levels (a) $g=4.0$, $u=0.12$, (b) $g=5.4$, $u=0.16$; (c) $g=6.4$, $u=0.19$; (d) $g=7.5$, $u=0.23$, (e) $g=11.4$, $u=0.34$, and (f) $g=17.3$, $u=0.53$; other parameters are fixed at $\beta=0.184$, $\beta_A=90$, and $R_1=R_2=4\%$.

IV. GENERAL DYNAMICAL FEATURES

In this section we consider more fully the dynamical features of stimulated scattering and their dependence on pump intensity and cavity reflectivity which are, from an experimental point of view, two main control parameters of the system. Pertinent to the experimental observations discussed below (Sec. V), the physical values we choose for these simulations correspond to typical values for SBS in fused silica fibers at 514 nm. These are [13,14] gain coefficient $g_B=2.6\times10^{-11}$ m/W, absorption coefficient $\alpha=4.6\times10^{-3}$ m^{-1}, nonlinear refractive coefficient (based on the electronic contribution), $n_2=2\times10^{-22}$ m^2/V^2, SBS gain bandwidth $\Delta\nu_B=143$ MHz, and effective cross sectional area $A_{\text{eff}}=20\,\mu m^2$.

A. Dependence of dynamics on pump intensity

For simplicity, we start by considering a weak pump intensity with fixed cavity reflectivities of 4% at either end of the medium, other parameters being held constant. This corresponds to an operating condition for which the intensity-induced nonlinear refractive effect is weak in the sense that it only moderates the phases of the fields and cannot generate dynamical output through interplay with the gain in the absence of external feedback. The interaction of the gain with the external feedback is therefore a dominant effect in promoting the dynamics. A typical temporal recording of the Stokes intensity is shown in Fig. 2(a), which shows similar qualitative features on a short-time scale to those in Ref. [11] in the sense that the oscillation is sustained with a basic frequency $\sim 1/2T_r$. However, a deep modulation superimposed on the profile is evident on a longer time scale, and more interesting, a two-wave alternating structure is also evident with a similar length scale to that of the modulation. These two waves transfer energy one to the other, the basic oscillating frequencies of the waves being the same $(1/2T_r)$, but with a time (phase) shift. This behavior appears to result from relative changes in the phases of pump, Stokes, and material waves during the interac-

tion process due to nonlinear refraction. The coupling conditions of the process therefore change, resulting in the scattered waves being either in phase or out of phase, thus exhibiting the alternating behavior. We note that this behavior appears only within a small region close to the threshold for stimulated scattering. On increasing the pump intensity it is largely suppressed and replaced by a sustained oscillatory mode with slow periodic modulation, Fig. 2(b). The sustained oscillations, again with basic frequency $1/2T_r$, comprise fine structures which overlap and compete with each other in regions within the period of the slow modulations [see inset of Fig. 2(b)]. These dynamical features remain essentially unchanged on increasing the pump intensity over a limited range except that the period of the slow modulation becomes progressively shorter [Fig. 2(c)]. For still higher pump intensity, as the modulation period approaches the basic frequency $1/2T_r$, the oscillatory dynamics become increasingly complex and random [Fig. 2(d)]. Beyond this pump intensity the sustained oscillatory behavior ceases and is replaced by a distinct bursting mode of operation. This seems to emerge from the sustained complicated oscillatory dynamics that collapses into intermittent bursts superimposed on a dc level of Stokes emission. We have observed various bursting pulses with durations up to $\sim 100T_r$ for appropriate parameter conditions, of which Fig. 2(e) is a typical example. The duration of the individual bursts of oscillation decrease and their separation increases on increased pumping, this trend leading to wider and wider temporal windows of stable dc emission. Further analysis shows a tendency for the bursting mode to predominate for longer medium lengths and also for higher feedback reflectivities, other parameters being held constant. We note that due to computational limitation it proved practically difficult to monitor a large number of bursting pulses, especially when their durations were long or they were widely separated as for conditions of high pumping. Consequently it remains to be determined whether the Stokes emission eventually becomes truly dc. In practice, however, our experiments show that the onset of higher-order effects, in particular second-order Stokes, occurs at the higher pump levels, the dynamical instabilities of which truncate the trend to dc of the first order Stokes emission.

The power spectra of the Stokes signals of these various dynamical forms show in general a basic frequency component, at $1/2T_r$, together with its harmonic orders. Fine structure evident in these spectra shows a number of close frequency peaks in the basic and harmonic components, confirming the dynamic frequency shifts arising from the nonlinear refractive effects as discussed earlier. Figure 3 shows a representative example of the power spectra corresponding to the data of Fig. 2(b). More generally, as expected, increasingly complex temporal structures exhibited more complicated frequency spectra, of increased spectral density. Such tendencies suggest that the bursting oscillations are a manifestation of many close lying frequency components, the relative phases of which determine the conditions for either constructive combinations (maximum signal) or destructive combinations (regions of no bursting) overlaying a dc background

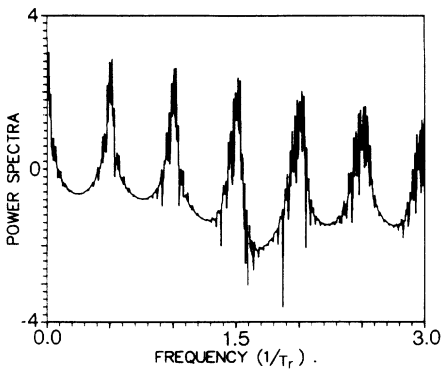

FIG. 3. Power spectrum of Stokes signal clearly showing the basic frequency component at $1/2T_r$, and its various harmonic orders. The quasiperiodicity of these components can be seen from their multipeak structure.

signal. The intermittency of the bursting modes and their random duration suggest that the frequency components and/or their phases are constantly changing with time. We note, however, that this argument is difficult to confirm by our spectral analysis due to its limited resolution.

B. Dependence of dynamics on reflectivity

By varying the cavity reflectivity, the feedback to the SBS interaction is changed. To ensure the validity of the approximation used to obtain the boundary conditions of Eq. (10), we restrict our considerations here to the limit of weak reflectivities. Extensive computational simulations have been done using various reflectivity values in this region, other parameters being held constant. Interestingly, for the fiber parameters we have chosen, we have so far not observed stable Stokes emission when the

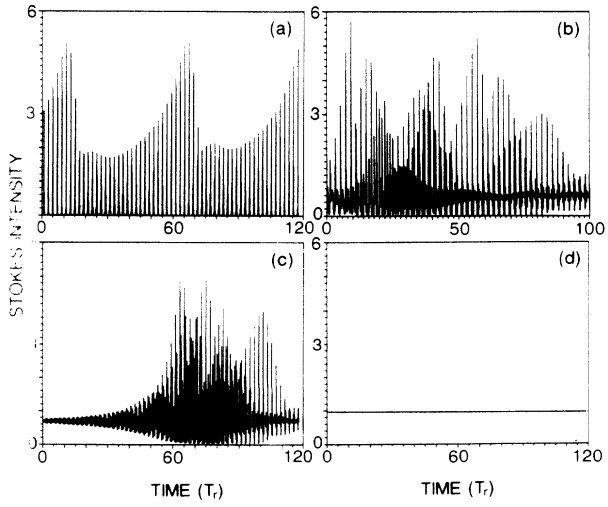

FIG. 4. Various dynamical forms of Stokes signal on increasing reflectivity from (a) $R_1=R_2=0.25\%$ to (b) $R_1=R_2=4\%$, (c) $R_1=R_2=9\%$, and (d) $R_1=R_2=36\%$. g and u are fixed at 8.7, 0.26, respectively, and other normalized parameters are set the same as in Fig. 2.

system operates in the region near to threshold for stimulated scattering, even when the reflectivity is much weaker than 4%. Rather it is always unstable once the pump intensity is high enough to generate stimulated scattering in the presence of the cavity. Such behavior in the Stokes intensity must therefore result from the feedback effect. Figures 4(a)-4(d) give a set of four temporal forms for different reflectivities (R_1,R_2) of 0.25%, 4%, 9%, and 36%, respectively, for a fixed pumping condition corresponding to $g=8.7$. They show, in order, sustained modulated oscillation of basic frequency $\frac{1}{2}T_r$ fast oscillation, a bursting mode, and eventually stable emission, at least over the time window of the numerics shown. By comparing this sequence with that in Fig. 2, similarity can be drawn between the data for increase of pump intensity and increase of cavity reflectivity. This may be understood physically since an increase of either results in a stronger nonlinear refraction.

V. EXPERIMENT

The experimental setup for the generation of stimulated scattering in an optical fiber, schematically shown in Fig. 5, is similar to that in Ref. [2]. The cw emission of a single-mode argon-ion laser at 514 nm, with an instantaneous linewidth of $\sim$15 kHz was used as a pump source providing variable output power stabilized to $\pm 2\%$. Two $10\times$ microscope objectives L_1 and L_2, were used to couple the light into and out of the optical fiber, respectively. The fiber comprised a pure SiO_2 core of diameter ~ 4.8 μm with a B_2O_3-doped SiO_2 cladding. It was optically isolated from the argon laser using a Faraday isolator (OFR Model No. IO-5-532) giving an isolation factor of 35 dB between them. The pump signal and backscattered signal, comprising, stimulated scattering together with residual linear scatter, were sampled via the beam splitter shown. These signals together with the signal transmitted through the fiber were detected using photodiodes (HP-type BPX65) D_1,D_2, and D_3 which have a rise time of <0.5 nsec. A transient digitizer (LeCroy TR8828C) having a data sampling rate of 5 nsec interfaced with a Masscomp computer (MC5600) was used for temporal recording and subsequent signal processing to provide power spectra. A Fabry-Pérot interferometer with variable spacer established the scattered signal to be stimulated Brillouin scattering throughout the range of pump intensities investigated, first-order Stokes emission prevailing over this range while the onset of second-order Stokes emission occurred at high pump intensities ($\geq$ three times above the threshold value for first-order Stokes generation).

When accurately cleaved normal to the fiber the natural reflectivity of the fiber ends (both $\sim$4%) provided a weakly bounded system. In other experiments a fully reflecting mirror was placed beyond but close to the rear end of the fiber, which in this instance was index matched, to provide a variable feedback by varying the distance of the mirror from the fiber and so the coupling efficiency of the reflected signal back into the fiber.

A. Dependence of dynamical features on pump power

Figure 6 shows a sequence of digitized temporal recordings (5 ns interval resolution) of the SBS output on increasing the pump power in a fiber length of 36 m with natural reflectivity. The pump power in the fiber ranged from 200 to 500 mW, the lower pump value being near the SBS threshold. Trace (a) shows an oscillatory wave train with a basic frequency of $1/2T_r$ and an irregular slow modulation; two-wave alternation is also evident. This dynamical mode existed only in a narrow window of pump power, immediately beyond which another form of

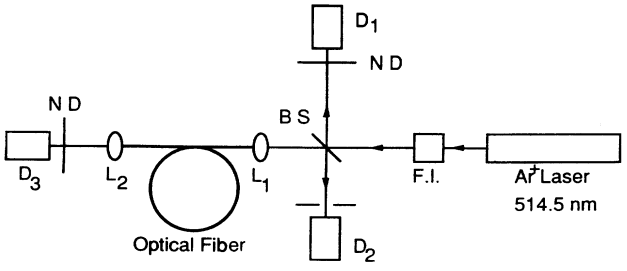

FIG. 5. Schematic setup of experimental arrangement. FI is Faraday isolator, ND neutral-density filters and D_1,D_2,D_3 are photodetectors.

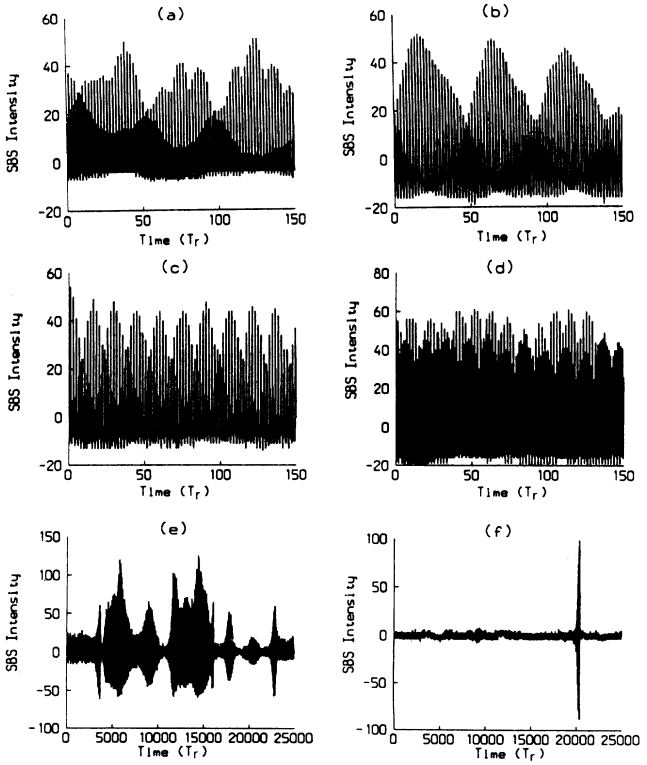

FIG. 6. Experimental observations of the dynamics of the Stokes SBS signal on increasing pump power P_{in} in fused silicon fiber of length 40 m and natural reflectivity, (a) and (b) $P_{in}\sim 250$ mW, (c) $P_{in}\sim 275$ mW, (d) $P_{in}\sim 380$ mW, (e) $P_{in}\sim 430$ mW, and (f) $P_{in}\sim 550$ mW.

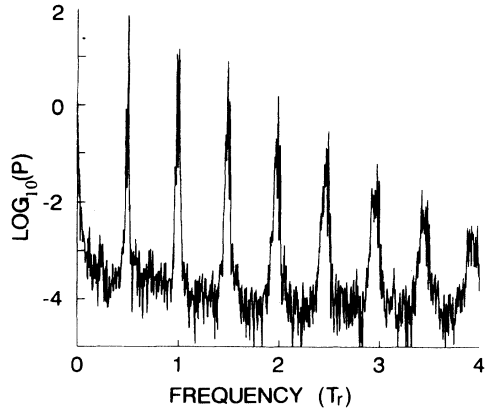

FIG. 7. Power spectrum of Stokes signal of date in Fig. 6(b).

oscillation with the same basic frequency but a regular slow modulation emerged as shown in Fig. 6(b). Overlap structure similar to that predicted in the theory is also seen in the valley region of the slow modulation. The corresponding power spectrum shows this motion to be quasiperiodic (Fig. 7), comprising a fine structure of multifrequency peaks in the basic and harmonic components. On increasing the pump level, the period of the regular modulation becomes shorter while other behavior remains essentially unchanged [Fig. 6(c)]. Faster and more complex fluctuations are evident at still higher pump levels [Fig. 6(d)]. These eventually divide into groups to form a random chain of bursting oscillations [Fig. 6(e)]. The duration of the individual bursts decreased while their separation increased [Fig. 6(f)] on increasing pump power further, finally leading to quasistable dc emission. We note that to catch the bursting signals [Figs. 6(e) and 6(f)], an alternative digitizer with an interval resolution of 320 ns was used providing a long-time window of ~ 5 ms in a full recording, though resulting in loss of high-frequency information.

B. Dependence of dynamical features on reflectivity

The influence of the cavity reflectivity on the dynamical behavior was studied by varying the position of the feedback mirror as discussed earlier. Theoretically the dynamical features in a weakly bounded system depend only on the product of the two reflectivities R_1 and R_2 rather than their individual values. Experimentally, the reflectivity R_1 at the entrance end was held fixed at its natural value, whereas R_2 at the exit end was varied. Figure 8 shows a series of experimental recordings for four different effective reflectivities with the pump power held constant. The effective reflectivity of the feedback mirror was calibrated as a function of its position in separate experiments by monitoring the reflected pump signal transmitted back through the fiber, the pump power being kept constant and below the threshold for SBS. The sequence shows, in order, low and fast sustained oscillations, bursting oscillations and stable emission, corresponding reflectivity R_2 being much lower, slightly lower, slightly higher, and much higher than 4%, respectively. These results are comparable with those ob-

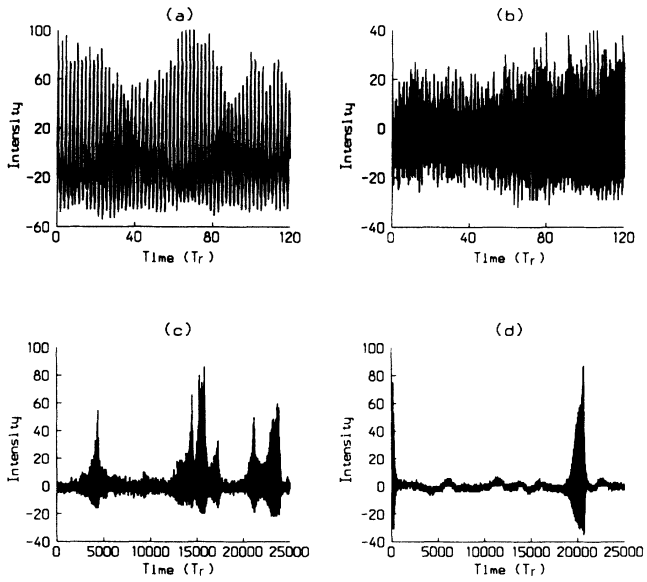

FIG. 8. Experimental observation of different dynamical behavior of Stokes signal on varying the cavity reflectivity $R_1 \sim 3.5\%$ (natural reflectivity) and (a) $R_2 \ll 4\%$, (b) $R_2 \leq 4\%$, (c) $R_2 \geq 4\%$, (d) $R_2 > 4\%$.

tained by our theory (Fig. 4) where R_1 $(=R_2)$ was chosen at 0.25%, 4%, 9%, and 36%.

VI. COMPARISONS AND DISCUSSION

Quantitative comparison of our theoretical predictions and experimental observations through Fig. 2 with Fig. 6, Fig. 3 with Fig. 7, and Fig. 4 with Fig. 8 shows obvious good agreement in regard to the detailed dynamical and quasistable features of the Stokes signal, their power spectra, and the dependence of these features on the two control parameters of pump power and cavity reflectivity.

In quantifying these comparisons, the parameter values for SBS have been properly chosen in our numerical simulations according to published data for fused silica fibers at 514 nm as given earlier. Accordingly for a fiber length of 40 m, our normalized parameter for Figs. 2(a)–2(f) correspond to pump power injections of 76, 102, 121, 143, 216, and 338 mW and those for Fig. 4 correspond to a pump power of 166 mW. Comparing these values with those of Figs. 6 and 8 for similar regions of dynamical behavior, the experimental values of pump intensity are greater by a factor of 2 approximately. Several reasons may be responsible for the difference. First the actual gain coefficient of the fiber used in the experiments is likely to be lower than the theoretical value used due to polarization scrambling effects in the nonlinear interaction, this effect resulting in an increase in the experimental SBS threshold, found to be the case from our comparisons. Second, while the maximum reflectivity at the fiber ends was measured to be 3.5%, the effective value may have been reduced if the fiber ends were not cleaved accurately normal to the fiber length, resulting in an increased pump power to produce similar dynamical behavior to our theoretical predictions based

on a value of 4%. Furthermore, the experimental fiber length was 10% shorter than that used in our simulations.

More general conclusions of the dependence of the dynamical forms of SBS on pump power, fiber length, and reflectivity have been obtained for a range of fiber length typically (25–100m). Experimental results show that the pump intensity for the onset of bursting and the subsequent trend to quasistable emission is reduced for longer fiber lengths and/or higher reflectivities. Theoretical comparisons for fiber lengths of 25 m and 40 m are in good agreement with these experimental findings.

In generalizing the results of our analysis to other types of stimulated scattering, we have further studied the dependence of the dynamics on the gain bandwidths of the stimulated scattering, characterized by the normalized parameter β_A. For a wide-gain bandwidth, as in stimulated Raman scattering (SRS), adiabatical elimination of the material equation is justified, the process now being governed by the pump and Stokes field equation only. General dynamical behavior in this case is found however to remain essentially unchanged. This can be understood since the bandwidth used for the SBS is already nearly wide enough to allow adiabatical elimination. On the other hand, for a narrow-gain bandwidth for which the material response time is accordingly slower, optical feedback from the material waves retains a longer memory which significantly changes the dynamics of the scattering processes. Our numerical analysis shows that in this region on decreasing β_A the modulated amplitude of the Stokes emission is progressively reduced and the dynamical features of the signal are significantly changed until the emission eventually becomes stable.

While the spatiotemporal behavior of stimulated scattering is evidently complex, the results of our analysis provide some qualitative insight into the underlying physical mechanism determining this behavior. Recalling first the work of Johnson and Marburger [3(a)] they showed stimulated scattering in an extended medium *without external feedback* to evolve to a steady state through relaxation oscillations comprising pulses of period equal to twice the transit time of the medium. Physically the $2T_r$ separation between successive peaks was attributed to the transit time T_r of the pump signal through the medium and the subsequent build up time T_r from noise of the counterpropagating scattered signal upon which the depleted pump signal in the medium was replenished in a further T_r time to then repeat the process. Our recent more generalized treatment of this problem [2] showed, however, that these features and their explanation only applied for conditions of weak amplification, for example, close to the pumping threshold, where the effect of nonlinear refraction may be neglected. More generally the emission was shown to exhibit complex sustained dynamics culminating in chaotic emission at higher pump levels.

In the present work we find that while the characteristic $2T_r$ period in the dynamics of the Stokes signal is reinforced by *external feedback,* the sustained dynamics beyond this transient regime become as before [2] strongly dependent not only on the SBS gain, and material relaxation time, but also the nonlinear refraction. Notably the characteristic modulation of the Stokes signal (see Figs. 2 and 6) appears to arise from time-dependent variation of the Stokes gain g, while this wave propagates in the medium. This results from time-dependent frequency shifting of the Stokes and pump signals induced by SPM and XPM through field-induced nonlinear refraction of the signals, the shift being most pronounced on the rising or falling regions of the fast oscillatory or pulsed features of these signals (those associated with the basic frequency $1/2T_r$). The implicit phase matching of the stimulated scattering interaction therefore becomes time dependent, the dynamic frequency shifts and intensities of these signals adjusting in a self-consistent way to maintain this condition, while the gain as seen by the Stokes signal varies in time according to the Stokes frequency shift from gain center. We have confirmed such effects to become increasingly pronounced as the gain bandwidth is reduced, dynamical frequency shifts for the typical pump intensities used in our analysis even being sufficient to move the frequency of the Stokes signal out of the bandwidth of the gain profile. Such effects also give rise to considerable distortion of the fast-pulsed features of the Stokes signal and commonly results in their splitting [inset Fig. 2(b)]. For the latter case multiwave structures emerge in the time series which compete with one another, and as we have seen earlier, these effects become stronger leading to increased temporal complexity on increasing the pump intensity, due to the increased gain-dispersive interaction. On the other hand, when a pulse component of the Stokes signal is poorly amplified as for example for pumping close to threshold or in the dynamic region when its frequency shift is large, the pump will be undepleted in the medium and so may lead to the emergence and growth of a secondary Stokes pulse. Our numerical simulations have confirmed this feature and show the satellite signals to generally occur around midway between the primary Stokes pulses of the pulse trains.

In conclusion, a reasonably complete theoretical description of stimulated scattering in the presence of low-reflectivity feedback has been presented. Theoretical results show the SBS signal to exhibit huge sustained or random bursts of quasiperiodic emission. Detailed comparisons with experimental findings give good agreement regarding both the temporal and stable features of the SBS emission and their dependence on the physical control parameters, e.g., pump power, cavity reflectivity, and fiber length. Significantly, our results confirm the essential role of nonlinear refraction to the dynamical behavior and suggest that the noise structure of the initial spontaneous Brillouin scattering has little influence in determining the behavior. From a practical point of view, the occurrence of dynamics over broad parameter regions, especially in the case of extremely small feedback, carries with it implication to the many technological applications of fiber systems.

ACKNOWLEDGMENTS

This work was jointly supported by the Science and Engineering Research Council (SERC) and the Air Force Office of Scientific Research (AFOSR, U.S.A.)

[1] See, for example, R. Shen, *The Principles of Nonlinear Optics* (Wiley, New York, 1984).
[2] (a) Weiping Lu and R. G. Harrison, Europhysics Lett. **16**, 655 (1991); (b) J. S. Uppal, Weiping Lu, A. Johnstone, and R. G. Harrison, in *Optical Society of America Proceedings on Nonlinear Dynamics in Optical Systems,* edited by N. B. Abraham, E. Garmire, and P. Mandel (Optical Society of America, Washington, D.C., 1991), Vol. 7, p. 558.
[3] (a) R. V. Johnson and J. H. Marburger, Phys. Rev. A **4**, 1175 (1971); (b) M. J. Damzen and H. Hutchison, IEEE J. Quantum Electron. QE-19, 7 (1983); (c) J. Coste and C. Montes, Phys. Rev. A **34**, 3940 (1986).
[4] S. M. Wandzura, in *Proceedings of the Conference on Lasers and Electro Optics, Anaheim, CA, 1988,* Vol. 7 of *1988 Technical Digest Series* (Optical Society of America, Washington, D.C., 1988), p. 8.
[5] E. M. Dianov, A. Ya. Karosik, A. V. Lutchnikov, and A. N. Pilipetoku, Opt. Quant. Electron **21**, 381 (1989).
[6] R. W. Boyd, K. Rzazewski, and P. Narum, Phys. Rev. A **42**, 5514 (1990).
[7] R. G. Harrison, J. S. Uppal, A. Johnstone, and J. V. Moloney, Phys. Rev. Lett. **65**, 167 (1990).
[8] A. Gaeta and R. W. Boyd, Phys. Rev. A **44**, 3205 (1991).
[9] A. Johnstone, Weiping Lu, J. S. Uppal, and R. G. Harrison, Opt. Commun. **81**, 222 (1991).
[10] K. Baumgartel, U. Motschmann, and K. Sauer, Opt. Commun. **51**, 53 (1984).
[11] I. Bar-Joseph, A. A. Friesun, E. Lichtaman, and R. G. Waarts, J. Opt. Soc. Am. B **2**, 1606 (1985).
[12] C. J. Randall and J. R. Albritton, Phys. Rev. Lett. **52**, 1887 (1984).
[13] G. P. Agrawal, *Nonlinear Fiber Optics* (Academic, New York, 1989).
[14] D. Cotter, Opt. Commun. **4**, 10 (1983).

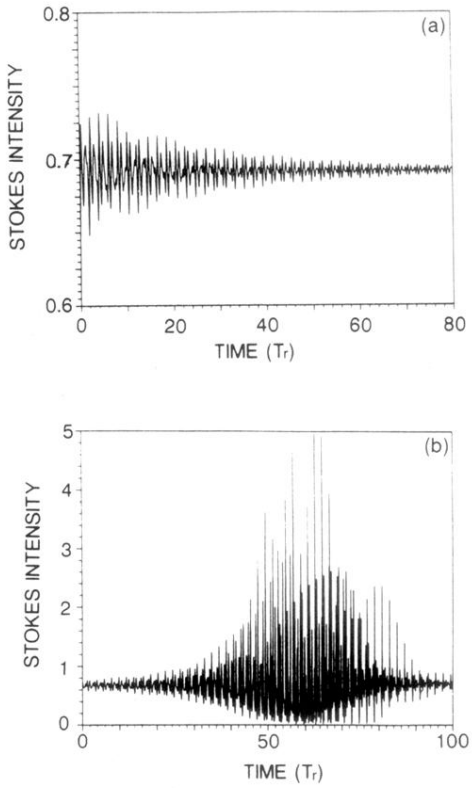

FIG. 1. (a) Relaxation oscillations of Stokes intensity, resulting from the interaction of gain with external feedback in the absence of refraction. (b) Bursting oscillation of Stokes signal in the presence of gain, refraction, and cavity feedback. The parameters are held at $g=11.4$, $\beta=0.184$, $\beta_A=90$, $u=0$, and $R_1=R_2=4\%$ with $u=0$ for trace (a) and $u=0.34$ for trace (b).

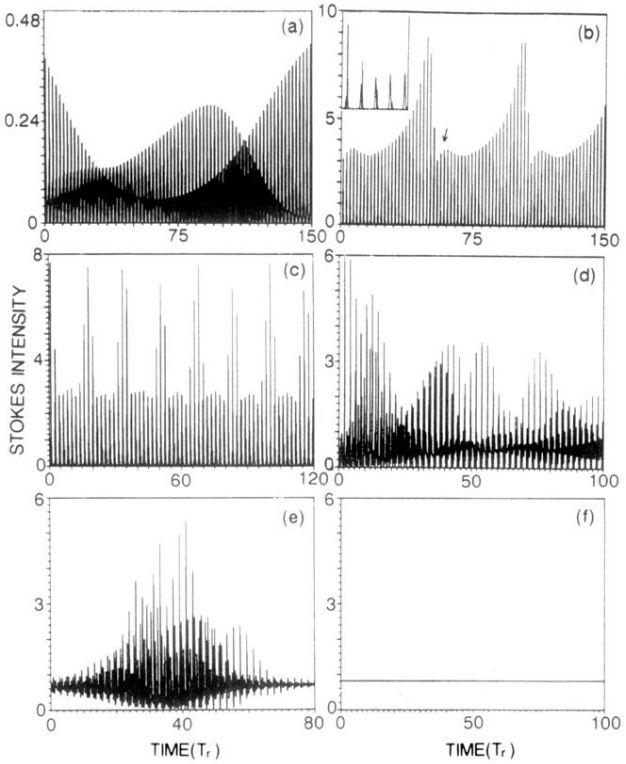

FIG. 2. A series of different dynamical features of Stokes signals on increasing pump power levels (a) $g=4.0$, $u=0.12$, (b) $g=5.4$, $u=0.16$; (c) $g=6.4$, $u=0.19$; (d) $g=7.5$, $u=0.23$, (e) $g=11.4$, $u=0.34$, and (f) $g=17.3$, $u=0.53$; other parameters are fixed at $\beta=0.184$, $\beta_A=90$, and $R_1=R_2=4\%$.

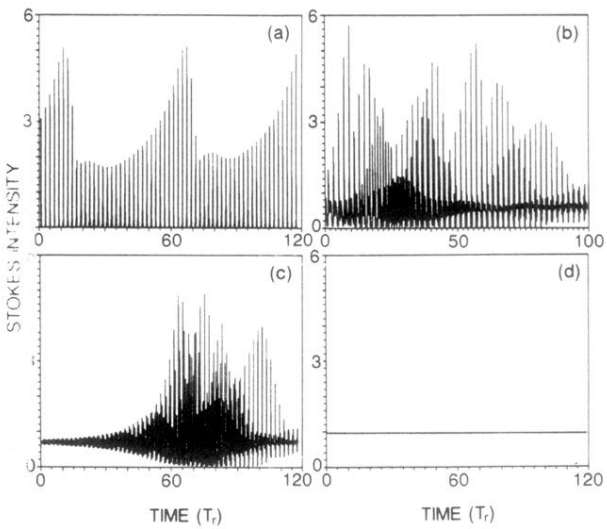

FIG. 4. Various dynamical forms of Stokes signal on increasing reflectivity from (a) $R_1=R_2=0.25\%$ to (b) $R_1=R_2=4\%$, (c) $R_1=R_2=9\%$, and (d) $R_1=R_2=36\%$. g and u are fixed at 8.7, 0.26, respectively, and other normalized parameters are set the same as in Fig. 2.

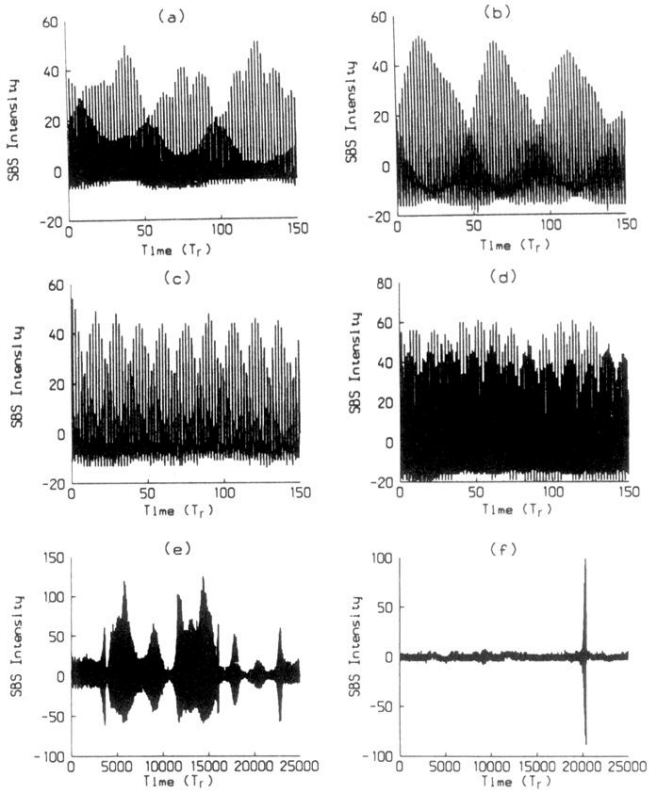

FIG. 6. Experimental observations of the dynamics of the Stokes SBS signal on increasing pump power P_{in} in fused silicon fiber of length 40 m and natural reflectivity, (a) and (b) $P_{in} \sim 250$ mW, (c) $P_{in} \sim 275$ mW, (d) $P_{in} \sim 380$ mW, (e) $P_{in} \sim 430$ mW, and (f) $P_{in} \sim 550$ mW.